PRAMANA — journal of physics
© Indian Academy of Sciences
Vol. 68, No. 4
April 2007
pp. 581–589

Phase knife-edge laser Schlieren diffraction interferometry with boundary diffraction wave theory

RAJ KUMAR[1], D MOHAN[2], SUSHIL K KAURA[1], D P CHHACHHIA[1] and A K AGGARWAL[1]
[1]Coherent Optics Division, Central Scientific Instruments Organisation, Sector 30, Chandigarh 160 030, India
[2]Department of Applied Physics, Guru Jambheshwar University of Science and Technology, Hisar 125 001, India
E-mail: aka1945@rediffmail.com; raj_csio@yahoo.com

MS received 22 November 2005; revised 25 September 2006; accepted 4 December 2006

Abstract. Within the framework of boundary diffraction wave theory it has been shown that the first bright fringe on either side of the central dark fringe of the phase knife-edge Fresnel diffraction pattern could be broadened to cover the whole field of view. Broadening of the first diffraction fringe, instead of conventionally modifying the spatial frequency spectrum, enhances the sensitivity of the Schlieren system. The use of phase knife-edge as viewing diaphragm in Schlieren diffraction interferometry not only enhances the fringe contrast but also avoids the loss in phase information as it lets through light from all parts of the test object and its thin interfacing makes the method suitable even for studying weak disturbances.

Keywords. Schlieren techniques; diffraction; phase visualization; optical testing techniques.

PACS Nos 42.79.Mt; 42.25.Fx; 42.25.Hz; 42.87.-d

1. Introduction

The plane wave-fronts in a beam of light gets distorted when they pass through a region of variable density, and as a result a variable phase distribution is produced in the exit plane, which is ordinarily invisible due to tremendous rapidity of optical oscillations. One of the simplest and widely used procedures to make these phase/index variations visible is the Schlieren technique [1–3]. In Schlieren techniques, the relative magnitude of phase gradients is estimated by slowly bringing the knife-edge towards the focal point and observing when an area becomes dark. The first areas to become dark will have positive gradients, followed by the flat areas and finally the negative gradients. Schlieren techniques can usually be used directly (i.e. without further processing) for a qualitiative/phenomenological description of the index variations and are often applied to heat and mass transfer phenomena, such as convection, mixing processes of gases or fluids, flame propagation phenomena, crystal growth monitoring, defect enhancement in periodic pattern, measurement of velocity fields of turbulent flows etc. [1–9] but not limited to these. Several modifications [1–4,10–13] have been reported in Schlieren techniques in a quantitiative manner where different viewing diaphragms have been used to enhance contrast and information content in the Schlieren interferogram. These techniques either provide low contrast in Schlieren interferogram or limit the test area or require specific complex viewing diaphragms or works in finite fringe mode where direct phase visualization becomes difficult, requiring further processing of the Schlieren interferogram. In conventional Schlieren diffraction interferometry [1–9], the Schlieren element (knife-edge, wire etc.) known as Schlieren stop blocks the Airy disk containing about 84% of the incident light, resulting in weak contrast of Schlieren interferogram.

Also, diffraction effects at the Schlieren stop impose the upper limit for the sensitivity of a Schlieren system. Recently [14,15], it has been shown that diffraction at Schlieren stop could gainfully be used to enhance the contrast and sensitivity of Schlieren diffraction interferometer. By using boundary diffraction wave theory, it has been demonstrated for the case of solid knife-edge [14] and mirror-edge [15] as viewing diaphragm that the first bright diffraction fringe near the geometrical shadow could be broadened so that it covers the field of view. At this position, Schlieren element diffracts light from the Airy disk instead of blocking it resulting in a relatively stronger diffracted reference beam thereby enhancing the contrast of Schlieren interferogram to provide finer details of the test object. Using the physically appealing boundary diffraction wave theory, which reduces Fresnel–Kirchhoff surface/double integral into a single line integral, instead of the generally used Fourier optics approach may simplify the process of calculating the light distribution in the Schlieren image/interferogram for quantitative analysis. In the present work, a $\lambda/2$ phase plate is used as a viewing diaphragm in the Schlieren set-up to diffract light from the Airy disk instead of just to modulate the spatial frequency spectrum [2,3,16,17]. For the case of phase knife-edge, the first bright fringe on either side of the central dark fringe of the Fresnel diffraction pattern could be broadened, by adjusting the diffracting aperture in proximity of the Schlieren focus, to cover the whole field of view for performing optical test studies on phase objects in a manner analogous to the well-known point diffraction interferometer [18,19]. The use of phase knife-edge instead of solid knife-edge or mirror-edge has the advantage that it allows information from every test point to image plane, providing complete information of the test object.

2. Principle and theoretical background

The proposed method is based on the known fact that diffraction pattern is due to interference of two superimposing waves [20]: the geometrical wave from the primary source of light (focus in our case) and the boundary diffraction wave from the secondary source (diffracting aperture). The observed diffraction fringe pattern starts broadening as the two contributing sources of light approach each other and ultimately results in an infinite fringe mode that could be used to study phase objects [14,15]. Further, in the case of a phase aperture, it has been shown that the boundary diffraction wave (BDW) is a combination of two diffracted waves, one from the free end and the other from the phase aperture end [21].

Reference to figure 1, a spherical wave $(A/r_{\mathrm{Q}})\ \exp(jkr_{\mathrm{Q}})$ is incident upon the x–y plane. Let us consider a constant phase jump $(k\Delta)$ between surfaces O and T of the plane x–y. The field of the incident wave can be represented as [21]

$$\begin{aligned} U(x,y,0) = (A/r_{\mathrm{Q}})\exp(jkr_{\mathrm{Q}}), &\quad Q \in O, \\ (A/r_{\mathrm{Q}})\exp\{jk(r_{\mathrm{Q}}+\Delta)\}, &\quad Q \in T. \end{aligned} \tag{1}$$

The total wavefield at point P_1(x, y, z) in the observation plane (OP) is

$$\begin{aligned} U(x,y,z) = (A/4\pi) \int\int_{\mathrm{O}} &\{\partial/\partial n[(1/r_{\mathrm{Q}})\exp(jkr_{\mathrm{Q}})](1/r)\exp(jkr) \\ &-(1/r_{\mathrm{Q}})\exp(jkr_{\mathrm{Q}})\partial/\partial n[(1/r)\exp(jkr)]\}\mathrm{d}x\mathrm{d}y \\ &+(A/4\pi)\int\int_{\mathrm{T}}\{\partial/\partial n[(1/r_{\mathrm{Q}})\exp(jkr_{\mathrm{Q}}+\Delta)](1/r)\exp(jkr) \\ &-(1/r_{\mathrm{Q}})\exp\{jk(r_{\mathrm{Q}}+\Delta)\}\partial/\partial n[(1/r)\exp(jkr)]\}\mathrm{d}x\mathrm{d}y. \end{aligned} \tag{2}$$

Applying the Maggi–Rubinowicz transformation, total field at observation point is [20]

$$U(x,y,z) = U^{(\mathrm{g})} + U^{(\mathrm{d})}, \tag{3}$$

where

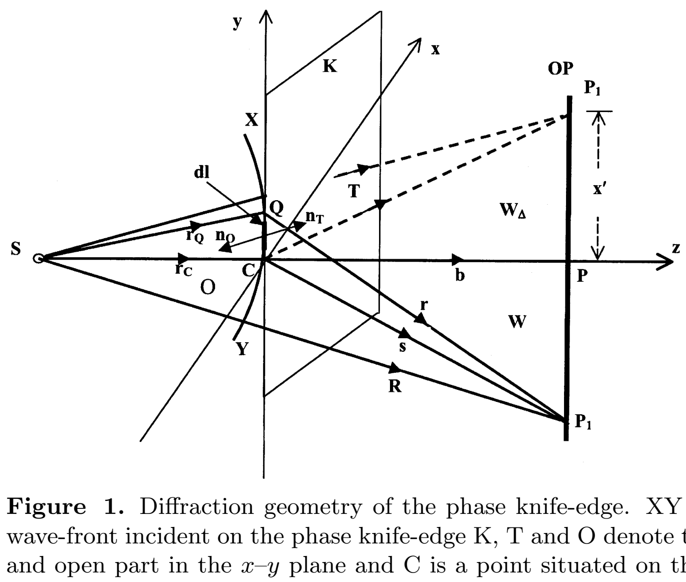

Figure 1. Diffraction geometry of the phase knife-edge. XY is a spherical wave-front incident on the phase knife-edge K, T and O denote the phase part and open part in the x–y plane and C is a point situated on the illuminated boundary of K.

$$
\left.\begin{array}{rll} U^{(\mathrm{g})} &= (A/R)\exp(jkR), & \text{when } P_1 \in W \\ &= (A/R)\exp[jk(R+\Delta)] & \text{when } P_1 \in W_\Delta \end{array}\right\} \tag{4}
$$

and

$$
\begin{aligned}
U^{(\mathrm{d})} &= U^{(\mathrm{d}')} + U^{(\mathrm{d}'')} \\
&= (A/4\pi)[1-\exp(jk\Delta)] \int_\Sigma \exp\{jk(r_\mathrm{C}+s)\}\cos(\mathbf{n}_\mathrm{O}, s) \\
&\quad \times \sin(r_\mathrm{C}, \mathrm{d}l)\mathrm{d}l/\{r_\mathrm{C}s[1+\cos(r_\mathrm{C}, s)]\},
\end{aligned} \tag{5}
$$

$$
\begin{aligned}
U^{(\mathrm{d}')} &= (A/4\pi) \int_\Sigma \exp\{jk(r_\mathrm{C}+s)\}\cos(\mathbf{n}_\mathrm{O}, s) \\
&\quad \times \sin(r_\mathrm{C}, \mathrm{d}l)\mathrm{d}l/\{r_\mathrm{C}s[1+\cos(r_\mathrm{C}, s)]\},
\end{aligned} \tag{6}
$$

$$
\begin{aligned}
U^{(\mathrm{d}'')} &= (A/4\pi) \int_\Sigma \exp\{jk(r_\mathrm{C}+s+\Delta)\}\cos(\mathbf{n}_\mathrm{T}, s) \\
&\quad \times \sin(r_\mathrm{C}, \mathrm{d}l)\mathrm{d}l/\{r_\mathrm{C}s[1+\cos(r_\mathrm{C}, s)]\},
\end{aligned} \tag{7}
$$

and

$$
\cos(\mathbf{n}_\mathrm{O}, s) = -\cos(\mathbf{n}_\mathrm{T}, s), \tag{8}
$$

where R is the length of the geometrical ray from source S to point P_1, Σ denotes the boundary of illuminated part of phase knife-edge (K), dl is an infinitesimal element situated on Σ and $\mathbf{n}_\mathrm{O}$ and $\mathbf{n}_\mathrm{T}$ are unit vectors orthogonal to r_C and dl. For simplicity the problem of phase knife-edge is studied in two steps. In the first step the problem is considered in all aspects as the problem of solid knife-edge and the second step is complimentary to it. Equation (5) shows that one does not have BDW whenever the phase jump is $2m\pi$ ($m = 0, 1, 2\ldots$). On the other hand, there is maximum contrast whenever the phase jump is $(2m+1)\pi$. This maximum value of contrast is twice that of a solid knife-edge. This is due to the fact that the BDW in the case of phase knife-edge differs from the solid knife-edge by a factor $[1-\exp(jk\Delta)]$. Here $U^{(\mathrm{g})}$ propagates according to the laws of geometrical optics and is known as the geometrical wave while $U^{(\mathrm{d})}$ is generated from every point of the illuminated boundary of the knife-edge and is called the boundary diffraction wave. The boundary diffraction wave can be split into three factors: (a) $A[1-\exp(jk\Delta)]\sin(r_\mathrm{C}, \mathrm{d}l)\mathrm{d}l/4\pi$ denotes the portion of incident wave which the edge element dl receives for diffraction, (b) $\exp(jks/s)$ expresses that diffracted wave originating from dl is a spherical wave, (c) the factor $\cos(\mathbf{n}_\mathrm{O}, s)/[1+\cos(r_\mathrm{C}, s)]$ is a directional factor due to which the spherical wave has an asymmetrical structure. It modulates the amplitude of the spherical wave.

If the point of observation (P_1) is very close to the reference point P, separating the geometrical shadow region from the directly illuminated region, one can safely approximate $\cos(r_\mathrm{C}, s) \sim 1$. Also when the knife-edge is close to focus, such that $r_\mathrm{C} \ll s$, and $r_\mathrm{C} + s \sim s$, eq. (5) reduces to

$$
\begin{aligned}
U^{(\mathrm{d})} &= (A/8\pi)[1-\exp(jk\Delta)] \int_\Sigma \exp\{jk(s)\} \\
&\quad \times \cos(\mathbf{n}_\mathrm{O}, s)\sin(r_\mathrm{C}, \mathrm{d}l)\mathrm{d}l/r_\mathrm{C}s.
\end{aligned} \tag{9}
$$

The above equation shows that the value of line integral over the boundary of diffracting aperture and the directionality factor $\cos(\mathbf{n}_{\mathrm{O}}, s)$ play an important role. It may be noted that in the case of knife-edge the value of Σ cannot be less than the diameter of Airy disk even for a diffraction-limited optics where the limiting value is $1.22\lambda F$ (F being the f-number of the focusing diffraction limited optics). Due to finite value of line integral and the directionality factor, the boundary diffraction wave is not spherical in the strict sense. In principle, one could, however, obtain a spherical diffracted wave in a situation where the diffracting aperture assumes point geometry, i.e. by using a tip or opaque disk having diameter less than half of the Airy disk diameter and positioned at its center. In fact this has been very elegantly achieved by Smartt and Steel [22] with a point-like diffracting aperture and by Furuhashi *et al* [23] with an opaque disk in the well-known point diffraction interferometer.

According to eq. (3) the irradiance distribution will be

$$\begin{aligned} I &= U(x,y,z)U(x,y,z)^* \\ &= |U^{(\mathrm{g})}|^2 + |U^{(\mathrm{d})}|^2 + C\cos(k\delta), \end{aligned} \tag{10}$$

where $C = (A^2/2\pi R)\int_\Sigma \cos(\mathbf{n}, s)\sin(r_{\mathrm{C}}, \mathrm{d}l)\mathrm{d}l/\{rs[1+\cos(s, r_{\mathrm{C}})]\}$ and δ is the optical path difference between two waves reaching the observation plane. It is well-known that the contrast of these fringes is not constant and goes on decreasing away from the boundary of the shadow, i.e. from the central dark fringe. This is because the amplitude of geometrical wave is almost constant while the amplitude of the boundary diffraction wave falls off rapidly with the distance from the boundary of shadow. It may also be noted that the fringe width of these fringes is not constant. Reference to figure 1, the value of the fringe width (β) for a case where knife-edge being close to focus, is

$$\beta = [2\lambda b^2/r_{\mathrm{C}}]^{1/2}[(n+1)^{1/2} - n^{1/2}], \quad n = 1, 2, 3, \ldots. \tag{11}$$

Equation (11) shows that the fringe width (β) goes on decreasing with increasing fringe order (n). Further, for a particular fringe order (n = constant), β can be increased by decreasing r_{C}, the distance between focus and the knife-edge, so that ultimately a single fringe covers the whole field of view. At this position, the system is adjusted for the infinite fringe condition where the boundary diffraction wave overlaps the geometrical wave and the two waves are either in phase ($k\delta = 0$, bright fringe) or out of phase ($k\delta = \pi$, dark fringe). This occurs when the knife-edge approaches the focus where it is difficult to distinguish the geometric wave from the boundary diffraction wave. Now a phase object ($\mathrm{O_b}$) having phase distribution $\exp(j\phi)$ interposed in any part of the collimated beam (figure 2) will refract light in a direction away from the main beam according to its phase variation. Most of this refracted light passes over the knife-edge without perturbation so as to form the geometrical wave and the irradiance distribution will be

$$I = |U^{(\mathrm{g})}|^2 + |U^{(\mathrm{d})}|^2 + C\cos(\phi). \tag{12}$$

It becomes obvious from eq. (12) that the intensity distribution of the interference pattern, in infinite fringe mode, depends on the phase variation (ϕ) introduced by the phase object ($\mathrm{O_b}$) into the test region between lenses $\mathrm{L_1}$ and $\mathrm{L_2}$. This shows

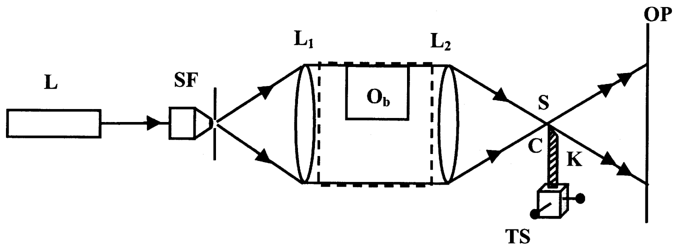

Figure 2. Schematic configuration of Schlieren diffraction interferometer.

that the described system behaves as a two-beam interferometer where interference takes place between an aberrated wave-front (test beam) and a reference wave-front (boundary diffraction wave).

3. Experimental details

The experimental arrangement of Schlieren diffraction interferometer is schematically shown in figure 2. The system consists of a light source (laser), two diffraction limited lenses and a diffracting aperture. A point source is created with a spatial filter assembly (SF) from a 35 mW He–Ne laser (wavelength = 633 nm, manufactured by Coherent, Inc.). The diverging laser beam is collimated by a well-corrected 100-mm-diameter, $f/4$ lens, L_1 (Tropel, Model 280, Laser Collimator). The shear plate interferometric technique was applied to ensure optical quality of the collimated beam. Another lens, L_2 (with same specifications as L_1) focuses the collimated beam to generate the source image. Here Ronchi ruling technique was used for the optical correction of light for astigmatism and coma, which would otherwise be introduced by the off-axis arrangement. This focused light upon divergence illuminates the phase knife-edge, K (a well-designed and properly fabricated $\lambda/2$ phase plate), mounted on a precisely controllable translation stage, TS. By providing fine movement to K, the distance r_{C} (figure 1) between knife-edge and the source (focus, S) is reduced so that the finite fringe mode interferogram ultimately converts to an infinite fringe mode interferogram. Experimentally, it has been achieved for the first-order bright fringe nearer to the central dark fringe by bringing the diffracting aperture close to the focus. The object O_{b} to be studied is interposed in the test region L_1L_2. The results presented here have been captured frame-by-frame with a Canon S-50 Power Shot digital camera (1024 × 768 pixels) to show the versatility of the set-up.

The phase knife-edge diffraction pattern in finite and infinite fringe mode is shown in figure 3. In the finite fringe mode, i.e. conventional diffraction pattern, alternate bright and dark bands of gradually decreasing contrast are observable on either side of the knife-edge position (central black fringe) while in infinite fringe mode the geometrical and BDW overlap each other and a single diffraction fringe covers the whole field of view. The central black fringe in finite fringe mode is formed because the counterpropagating components of BDW (i.e. those propagating in the directly illuminated region and in the geometrical shadow region) have equal

(a) (b)

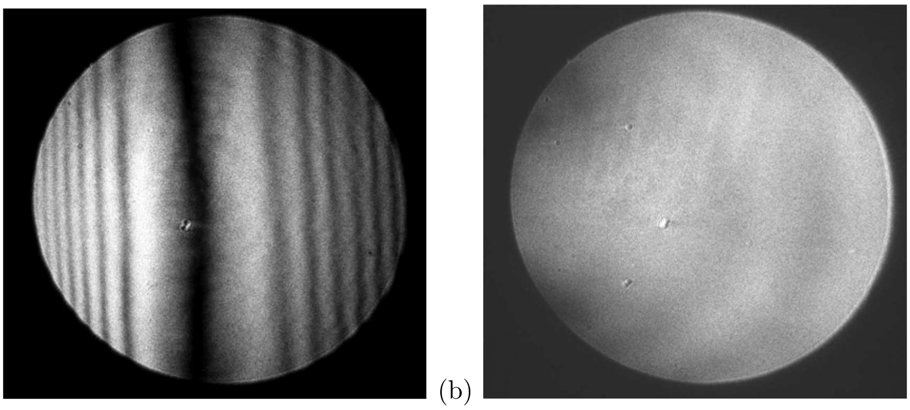

Figure 3. Photograph of typical diffraction pattern of phase knife-edge. (**a**) Finite fringe mode, (**b**) infinite fringe mode.

(a) (b)

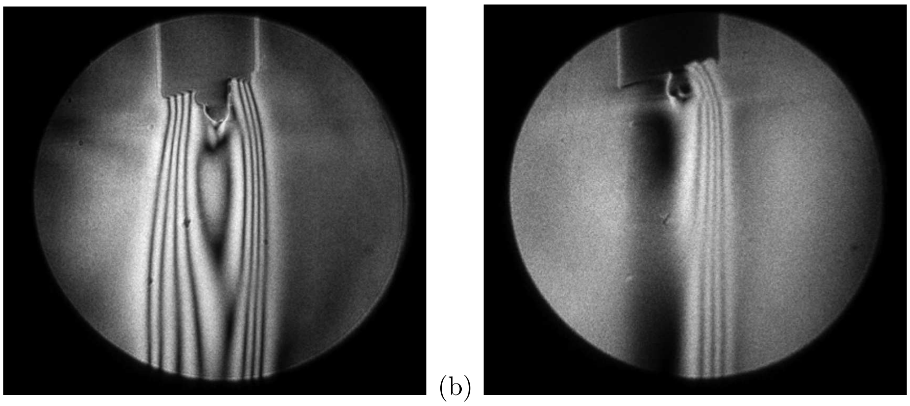

Figure 4. Photograph of typical interference pattern of a burning candle in infinite fringe mode (**a**) with phase knife-edge and (**b**) with solid knife-edge.

intensity but opposite phase, these components interfere destructively in a line corresponding to the opto-geometrical image of the edge [24]. Figure 4a presents the phase knife-edge test results in infinite fringe mode as a burning candle is interposed in the test region whereas figure 4b depicts the corresponding results of a solid knife-edge. It is obvious from these results that in the case of phase knife-edge, complete detailed information about the test object becomes available, which is not possible in the case of a solid knife-edge or mirror-edge where half of the information is blocked. It may be noted that the fringe contrast also gets enhanced due to doubling of the amplitude of the diffracted wave, providing finer information of the test object. Still the information is not completely true as the knife-edge diffraction interferometry provides information about transverse refractive gradients. However, complete information could be obtained from a series of photographs taken with a phase knife-edge rotated to various positions [4].

4. Conclusions

The physically appealing theory of diffraction: the boundary diffraction wave theory is used to explain the Schlieren diffraction interferometry with a phase knife-edge as the viewing diaphragm. It has been shown theoretically as well as experimentally that use of a $\lambda/2$ phase plate enhances contrast of Schlieren interferogram which is double to that of solid knife-edge and is equal to the mirror-edge Schlieren diffraction interferometer. Diffracting light from the Airy disk instead of just modulating the spatial frequency spectrum gainfully utilizes the diffraction at viewing diaphragm to improve the sensitivity of the system. Phase knife-edge as viewing diaphragm also avoids the loss of phase information occurred for the case of solid knife/mirror-edge because it lets through light from all parts of the test object to the observation plane, making the method suitable even for studying weak disturbances. The intensity, contrast and ease of production of the Schlieren interference pattern created by the laser beam were found to be remarkable.

Acknowledgements

The authors are grateful to the Director, CSIO, Chandigarh for his constant encouragement, support and for permission to publish this work. They wish to thank Mr A K Sharma for helpful discussions throughout the work and to Council of Scientific & Industrial Research, New Delhi for financial support (Emeritus Scientist Scheme).

References

[1] G S Settles, *Schlieren and shadowgraph techniques: Visualizing phenomena in transparent media* (Springer-Verlag, Berlin, 2001)
[2] D Malacara (Ed.), *Optical shop testing*, 2nd ed. (Wiley, New York, 1992), Chap. 8, pp. 299–309
[3] L A Vasil'ev, *Schlieren methods* (Wiley, New York, 1971)
[4] E B Temple, *J. Opt. Soc. Am.* **47**, 91 (1957)
[5] A Srivastava, K Muralidhar and P K Panigrahi, *Appl. Opt.* **44**, 5381 (2005)
[6] E Garbusi, J A Ferrari and C D Perciante, *Appl. Opt.* **44**, 2963 (2005)
[7] F Croccolo, D Brogioli, A Vailati, M Giglio and D S Cannell, *Appl. Opt.* **45**, 2166 (2006)
[8] H Kleine, H Gronigb and K Takayama, *Opt. Lasers Eng.* **44**, 170 (2006)
[9] D R Jonassen, G S Settles and M D Tronosky, *Opt. Lasers Eng.* **44**, 190 (2006)
[10] J Stricker and F Rosebblatt, *Opt. Lett.* **28**, 1427 (2003)
[11] L Joannes, F Dubois and J C Legros, *Appl. Opt.* **42**, 5046 (2003)
[12] B Zakharin and J Stricker, *Appl. Opt.* **43**, 4786 (2004)
[13] R Kumar, D P Chhachhia and A K Aggarwal, *J. Opt. A: Pure Appl. Opt.* **8**, 747 (2006)
[14] R Kumar, S K Kaura, A K Sharma, D P Chhachhia and A K Aggarwal, *Opt. Laser Technol.* **39**, 256 (2007)
[15] R Kumar, D P Chhachhia and A K Aggarwal, *Appl. Opt.* **45**, 6708 (2006)

[16] R Barakat, *J. Opt. Soc. Am.* **59**, 1432 (1969)
[17] M C Simon, J M Simon and E L de Zenobi, *Appl. Opt.* **18**, 1463 (1979)
[18] A K Aggarwal and S K Kaura, *J. Opt. (Paris)* **17**, 135 (1986)
[19] J S Goldmeer, D L Urban and Z Yuan, *Appl. Opt.* **40**, 4816 (2001)
[20] M Born and E Wolf, *Principles of optics*, 6th edn (Pergamon, Oxford, 1991), pp. 449–453
[21] S Ganci, *J. Opt. Soc. Am.* **A3**, 2094 (1986)
[22] R N Smartt and W H Steel, *Jpn. J. Appl. Phys. Suppl.* **14-1**, 351 (1975)
[23] H F Furuhashi, A Shibata, Y Uchida, K Matsuda and C P Grover, *Opt. Commun.* **237**, 17 (2004)
[24] P V Polyanskii and G V Polyanskaya, *J. Opt. Technol.* **64**, 321 (1997)